The Journal of the Korean Society of Oceanography
Vol. 31, No. 1, pp. 23-31, March 1996

A Simple Model of the Formation of Thermo-haline Front in the Southeastern Yellow Sea in Winter

YOUNG HO SEUNG AND SANG-IK SHIN
Department of Oceanography, Inha University, Incheon, 402-751, Korea

The thermo-haline front frequently observed near the southwestern tip of Korean Peninsula is successfully modeled using a simple model. The front is formed by the wind-driven advection of local cooled water to the southern warm area which is kept warm by large heat advection of the Tsushima Current. The front thus locates north of the Tsushima Current which runs approximately along the isobaths in the east-west direction.

INTRODUCTION

The Yellow Sea is a shallow embayment enclosed by Chinese continent and Korean Peninsula on the western edge of the North Pacific Ocean (Fig. 1). The northern part of the basin north of the Shantung Peninsula is usually called the Pohai. The water depth in the Yellow Sea is less than 90 m. A deep trough runs in roughly north-south direction and is nearer to the Korean side. In winter, dry, cold arctic continental air mass outbreaks from the north and cools the thin water column making it vertically homogeneous. In summer, a shallow thermocline forms due to the strong solar radiation. This thermocline plays the role of insulator allowing the water below the thermocline to remain cold. The cold water is referred to as the Yellow Sea Bottom Cold Water (c.f., Nakao, 1977).

Since Uda(1934), it has been believed that a current called the Yellow Sea Warm Current exists in the Yellow Sea. Current measurements (KORDI, 1987) show, however, no indication of persistent circulation except strong tidal currents and some episodic currents probably related to strong local winds. Later, it is known that a warm current turns clockwise around Cheju Island toward the Korea Strait further east (Park, 1986a; Chang *et al*, 1995). This current is known as the western edge of the Tsushima Current which is believed to be separated from the Kuroshio and modified by interacting with local coastal waters (Lim, 1971); The main part of the Kuroshio remains off the continental shelf and flows along the continental slope (Nitani, 1972). The Tsushima current is not known to enter the Yellow Sea in summer (Park, 1986a; Chang *et al*, 1995). Recent current observations (Hsueh, 1988) provide evidence of warm water intrusion in winter, which fact has long been conjectured from the historical data (e.g., Fig. 2) and satellite infrared images (e.g., Zheng and Klemas, 1982). Observations by Hsueh (1988) show that the northward upwind intrusion along the trough is due to the southward rise of sea level by the prevailing north wind pulse in winter. They also show that downwind current is induced over the shallow coastal areas. A simple model of the mean upwind current (Park, 1986b) also shows that the upwind current is dominated by pressure gradient and the downwind current, by wind stress. Due to the presence of Shantung Peninsula, however, this mean upwind current seems to be deflected westward (Seung, 1995), which otherwise is in northward direction.

A thermo-haline front is frequently observed in winter near the southeastern corner of the Yellow Sea (e.g. Fig. 2), i.e., southwestern tip of Korean

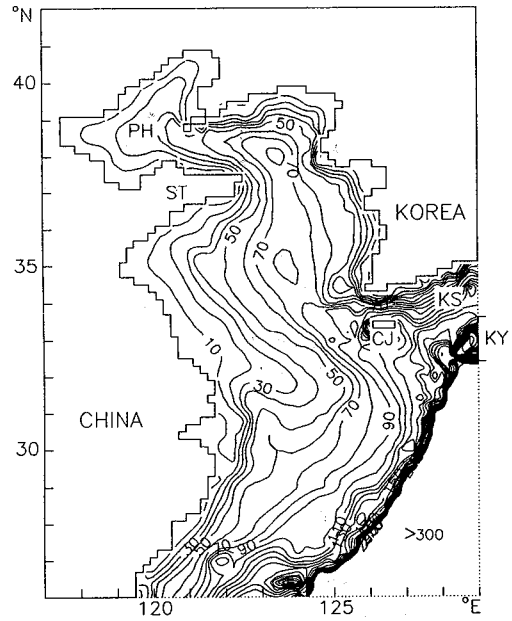

Fig. 1. Model domain and bottom topography (in meter) for the area shallower than 300 m. PH means Pohai, ST Shantung Peninsula, CJ Cheju Island, KS Korea Strait, KY Kyushu Island. Open boundaries are denoted by dottted lines.

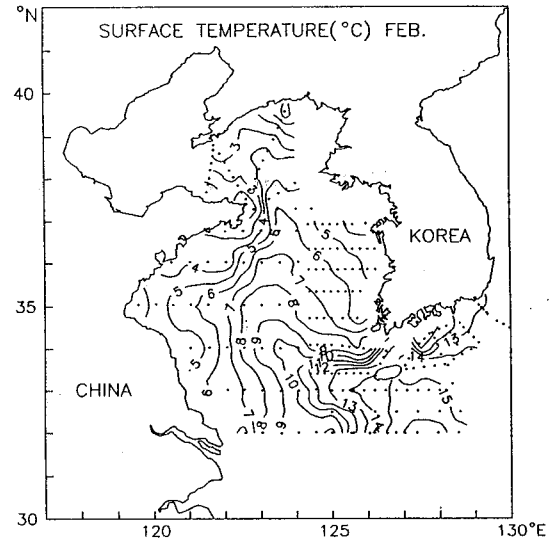

Fig. 2. Climatological mean surface temperature in February. Data are from Ministry of Sciences and Technology (1993 and 1996). Dots are data points.

Peninsula (Nakao, 1977; Lie, 1985; Chang *et al*, 1995). However, the formation mechanism of this front has not been extensively investigated. This front separates the warm saline water in the south just outside the basin from the cold fresher water in the north just inside the basin. The former is the nearby passing Tsushima Current Water and the latter is the local water mass cooled by surface heat flux. The front runs along the east-west direction just south of 34°N within the longitudinal range of 124° - 126° E (Fig. 2). It is interesting to remark that this front occurs approximately parallel to the isobaths (Fig. 1). While the intrusion of warm water is largely blocked in the eastern half of the basin by the presence of the front, the western half is largely affected by the warm water which intrudes north/northwestward into the basin (Fig. 2).

In this paper, an attempt is made to explore the formation mechanism of this front by using a simple model. Advection of heat and salt by current is hypothesized to be the major factor and examined with the assumption that temperature and salinity behave like passive tracers: i.e., the dynamics of the front is independent of the detailed density structure near the front. This assumption is based on the fact that the substantial temperature and salinity gradients across the front compensate each other such that the density contrast is greatly reduced (Lie, 1985). Steady current field in this region has already been modeled by Hsueh (1986) but no rigorous discussions have been given. In the following sections, velocity field is first obtained, and is used in determining the temperature field. The temperature field then is compared with the observed one. Finally, the formation mechanism of the front is discussed.

CURRENT FIELD

The steady, linearized, shallow water equations of motion and continuity are, respectively,

$$-fv = gh_x + \frac{\tau^x}{\rho d} - \frac{ru}{d} \tag{1}$$

$$fu = -gh_y + \frac{\tau^y}{\rho d} - \frac{rv}{d} \tag{2}$$

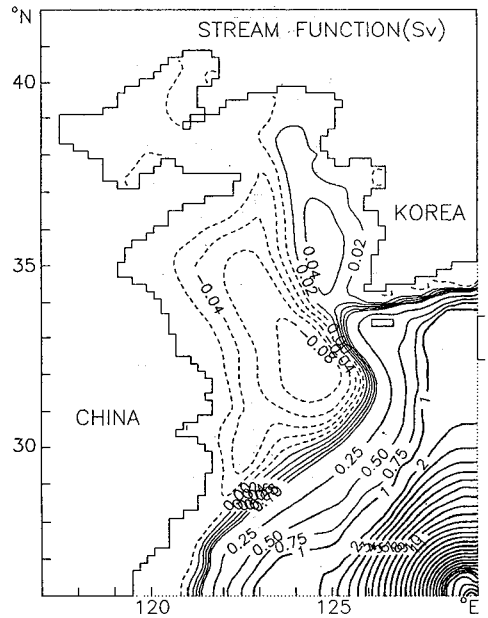

Fig. 3. Distribution of stream functions obtained in the model for Tsushima Current transport 1.5 Sverdrup. Dotted and solid contours are, respectively, for positive and negative values. Contour intervals are 0.02 from 0.0 to 0.1, 0.25 from 0.25 to 1.0 and 1.0 from 1.0 to 30 Sverdrups. Others are the same as Fig. 1.

$$(ud)_x + (vd)_y = 0 \tag{3}$$

where (x, y) point respectively, eastward and northward directions, (u, v) velocity components in (x, y) directions, h the sea surface elevation, f the Coriolis parameter, r the bottom friction coefficient, d the bottom depth, (τ^x, τ^y) the wind stresses in (x, y) directions, ρ the density of water and g the gravitational acceleration. Subscripts denote partial differentiation. From (3), a transport stream function ψ can be defined by

$$ud = -\psi_y, \quad vd = \psi_x \tag{4}$$

Using (4), the sea surface elevation can be eliminated from (1) and (2). For uniform northerly wind stress, the result is

$$\psi_{xx} + \psi_{yy} - \left(2\frac{d_x}{d} + f\frac{d_y}{r}\right)\psi_x - \left(2\frac{d_y}{d} - f\frac{d_x}{r}\right)\psi_y - \frac{\tau^y}{\rho r}d_x = 0 \tag{5}$$

Equation (5) is solved numerically, using the scheme developed by Fiadeiro and Veronis (1977), for the modeling domain shown in Fig. 1. Typical wind stress is taken as $\tau^y = -0.1$ N/m^2 (c.f., Hsueh, 1988). It is found that employing different values of wind stress, without changing the order of magnitude, does not significantly modify the current pattern: Corioilis parameter f is taken as 8.36×10^{-4} sec^{-1}, the water density as 1000 kg/m^3 and the friction coefficient as 0.002. For the same reason as that described in Hsueh *et al.* (1986), equivalent barotropic depth is taken as 300 m for the area deeper than 300 m. Most part of the modeling domain, including the area of main interest, has bottom depth smaller than 300 m. In this area, barotropic model seems appropriate in winter because of the homogeneity of the water columns in winter. Along the eastern open boundary, 30 Sverdrups of transport are allowed to flow out normal to the boundary: 1.5 Sverdrups by the Tsushima Current through the Korea Strait and 28.5 Sverdrups by the Kuroshio main stream through the region south of Kyushu (see Fig. 1 for locations). Thses values of transport are only approximate ones (c.f., Nitani, 1972; Moriyasu,1972; Qiu and Imasato, 1990) because exact transport values are not yet known. However, the Tsushima Current is believed to have transport less than 3 Sverdrups. Along the southern open boundary, 30 Sverdrups of transport are allowed to flow in normal to the boundary. Since the flows are restricted only normal to the open boundaries, specific values of stream function along the open boundaries are internally determined. Different values of the Tsushima Current transport are also considered later because the transport imposed by the inflow-outflow, being much larger than that by the local wind, is expected to greatly affect the circulation in the Yellow Sea.

The model result in Fig. 3 shows that the western edge of the Tsushima Current turns around Cheju Island toward the Korea Strait, apparently along the isobathic lines, as observed (c.f., Park, 1986a; Chang et al, 1995). A small portion of it enters the Yellow Sea, turns around the outer rim of the anticyclonic gyre east of the trough and rejoins the

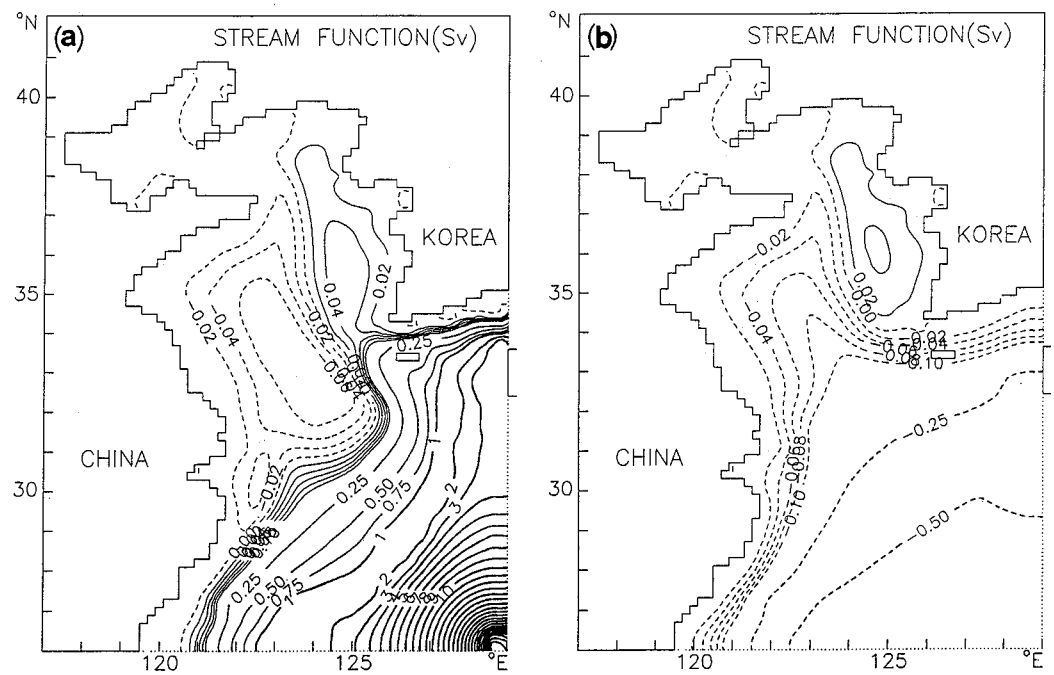

Fig. 4. Distribution of stream functions in cases where a) the Tsushima Current transport is 3.5 Sverdrup and b) there is no Kuroshio/Tsushima Current. Others are the same as Fig. 3.

Tsushima Current. Interestingly, this fact is compatible with the observational result (Cho and Kim, 1994; Wells and Huh, 1984) that there is an intrusion of water mass from the west to the south along the Korean coast. Differently from the circulation east of the trough, the cyclonic gyre west of the trough is entirely isolated from the open sea by the Tsushima Current. The main stream of the Kuroshio, off the continental shelf, may not seem realistic because of the unrealistic conditions. It is, however, reminded that our interest lies inshore of the continental slope.

A series of experiments with various inflow-outflow conditions indicates that the circulation east of the trough becomes more affected by the Tsushima Current as the transport of the Tsushima Current increases. For transport more than 3 Sverdrups, the closed form of streamline disappears (e.g., Fig. 4a). In reality, this case may not happen because the Tsushima Current is generally believed to have transport less than 3 Sverdrups. It seems that as the current becomes stronger by the increased effect of the Tsushima Current, it tends more to follow the isobathic lines (compare the stream lines in Fig. 4a with isobaths in Fig. 1 in the area under consideration). In fact, stronger current needs only smaller deviation from the isobathic lines to obtain the same vortex stretching effect as that obtained by larger deviation of weaker current. As noted in Seung(1995), current tends to have vortex stretching by flowing into deeper water in order to counterbalance the negative torque exerted by northerly wind blowing over the sea surface with bottom depth sloping up eastward. Without the inflow-outflow through the open boundaries (flows are assumed normal to the open boundary as mentioned above), i.e., without the Kuroshio/Tsushima Current, the anti-cyclonic gyre becomes completely isolated from the open sea whereas the cyclonic circulation becomes open at the southern and eastern open boundaries (Fig. 4b). The upwind transport is thus supplied by the westward Ekman drift coming through the eastern open boundary and the downwind tran-

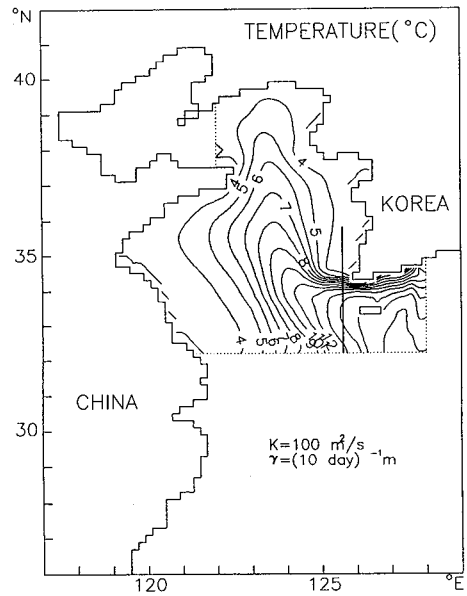

Fig. 5. Distribution of isotherms obtained in the model for the standard case, i.e., with the Tshushima Current transport 1.5 sverdrup, diffusion coefficient $K = 100$ m^2/s and cooling coefficient $\gamma = (10\ \text{day})^{-1}$ m. A thick line is drawn across the front along which temperature changes are examined. Dotted lines are model open boundaries.

sport along the Chinese coast leaks out through the southern open boundary.

TEMPERATURE FIELD

A passive tracer can be introduced into the obtained velocity field and allowed to freely advect with some diffusion and local cooling. Temperature is taken as the tracer concentration. As mentioned earlier, temperature and salinity compensate each other such that the resulting density is nearly uniform in the area of interest. Since salinity goes out of phase with temperature, consideration of only the latter suffices, i.e., distribution of the former can be inferred from that of the latter. The governing equation is

$$\psi_y T_x - \psi_x T_y + \left(dKT_x\right)_x + \left(dKT_y\right)_y - \gamma\left(T - T^*\right) = 0 \qquad (6)$$

where T is the temperature and K is the diffusion coefficient. To reflect the effect by local cooling, a newtonian damping term may be employed with coefficient γ and reference temperature T^*. Along the solid boundaries, no heat flux condition is applied. Along the open boundaries, measured temperatures are imposed. Since the measured temperature data (Fig. 2) are not available for the whole domain, the original domain is much reduced so as to it can be covered by the measured data. With these conditions, equation (6) is numerically solved, using again the scheme by Fiadeiro and Veronis (1977), for the new domain. The obtained velocity field shown in Fig. 3 is used.

In solving (6), the diffusion coefficient is taken as $K = 100$ m^2/sec, cooling coefficient as $\gamma = (10\ \text{day})^{-1}$ m and reference temperature as 3°C. The reference temperature used here is the mean winter air temperature in this region. We define the case considered here as 'standard' because either the values of parameters involved in it seem reasonable or it gives the most realistic result. Dependence of the model results on the diffusion and cooling coefficients and the Tsushima Current transport is discussed later. Despite the simplicity of the model, the resemblance of the computed temperature field (Fig. 5) to the observed one (Fig. 2) is encouraging. Particularly, the thermo-haline front and the tongue-shaped distribution of isotherms showing the intrusion of warm water into the basin are successfully reproduced. By comparing the current and temperature fields, Fig. 3 and 5, it is learned that the tendency for the isotherms to follow the streamlines depends on the strength of the current. The same reasoning as that taken above for the vorticity tendency can be applied here: stronger current needs only smaller deviation from the isothermal lines to obtain the same effect of advection as that obtained by larger deviation of weaker current.

To examine the dependence of the model on the diffusion and cooling coefficients, various coefficients are attempted. It is found that the fundamental character of the temperature distribution pattern is relatively insensitive to these coefficients

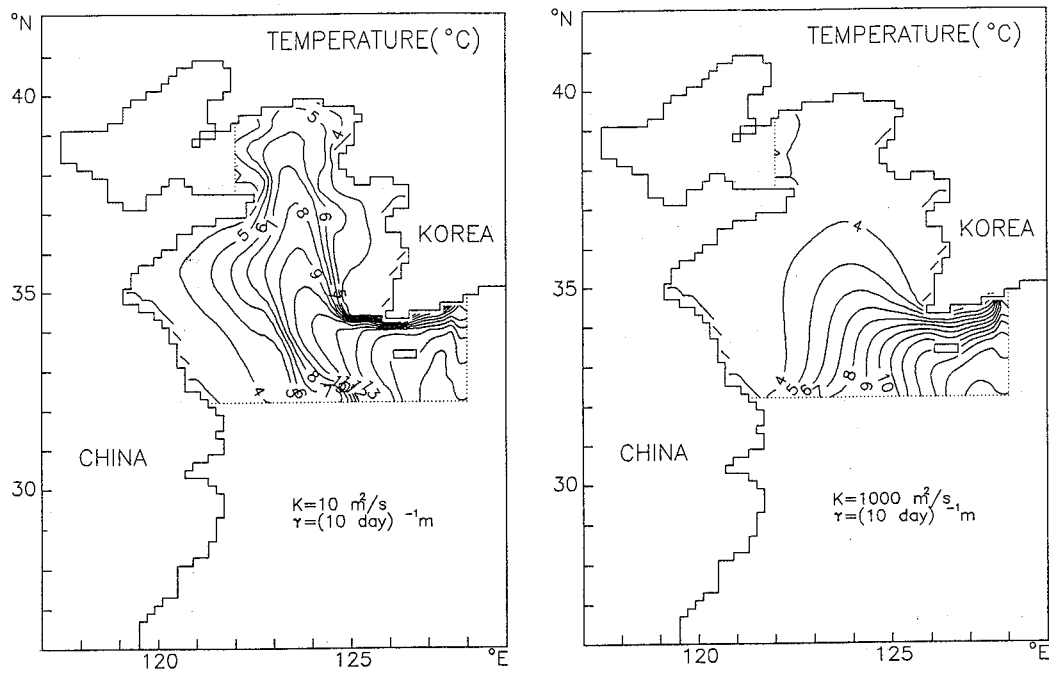

Fig. 6. Distribution of isotherms obtained in the model with diffusion coefficients $K = 10$ m^2/s and 1000 m^2/s. Others are the same as Fig. 5.

(Fig. 6 and Fig. 7). The velocity field applied to the heat equation (6) is that for 1.5 Sverdrups of the Tsuhsima Current transport. For comparison, various velocity fields obtained earlier are also applied. In all these cases, the thermo-haline front persists (e. g., Fig. 8a and 8b). However, more intense front results by the presence of the Tsushima Current. No significant difference is remarked between the cases for 1.5 Sverdrup (Fig. 4) and 3.5 Sverdrups (Fig. 8a) of Tsushima Current transports. It seems that the Tsushima Current, much stronger than the local wind-driven current within the basin, advects large amount of heat, keeps the region warm and therefore maintains the front.

To understand further the formation mechanism of the thermo-haline front, the magnitudes of various terms in heat equation (6) are obtained for the standard case (Fig. 5) along the line crossing the front. The results are shown in Fig. 9. It is found that, outside the frontal region, especially in the south, advection is most important in determining the temperature field. In fact, the heat advection by the strong Kuroshio and Tsushima Current may be dominant as noted above. Diffusion acts mostly in the north-south direction and is important only near the frontal region. The local cooling appears to be of minor importance. There is a heat loss by advection near the northern border of the front and a heat gain by advection near the southern border. These heat changes are mostly due to the advection in y-direction and balanced by north-south diffusion. Considering that diffusion plays only a passive role in the heat equation, the front in this model is initiated by advection. Close examination of the velocity field (Fig. 3) and the resulting temperature field (Fig. 5) indicates that the front occurs north of the strong Tsushima Current region. This may be because, as noted above, the strong (warm) current has a dominant effect on the temperature distribution by large heat advection. It leaves warm water behind and thus keeps the region warm. As observed in the previous section (Fig. 3), part of the downwind current along the Korean coast turns offshore forming the closed recirculation but the remaining part in nearshore area continues to flow along the coast by turning eastward. The former

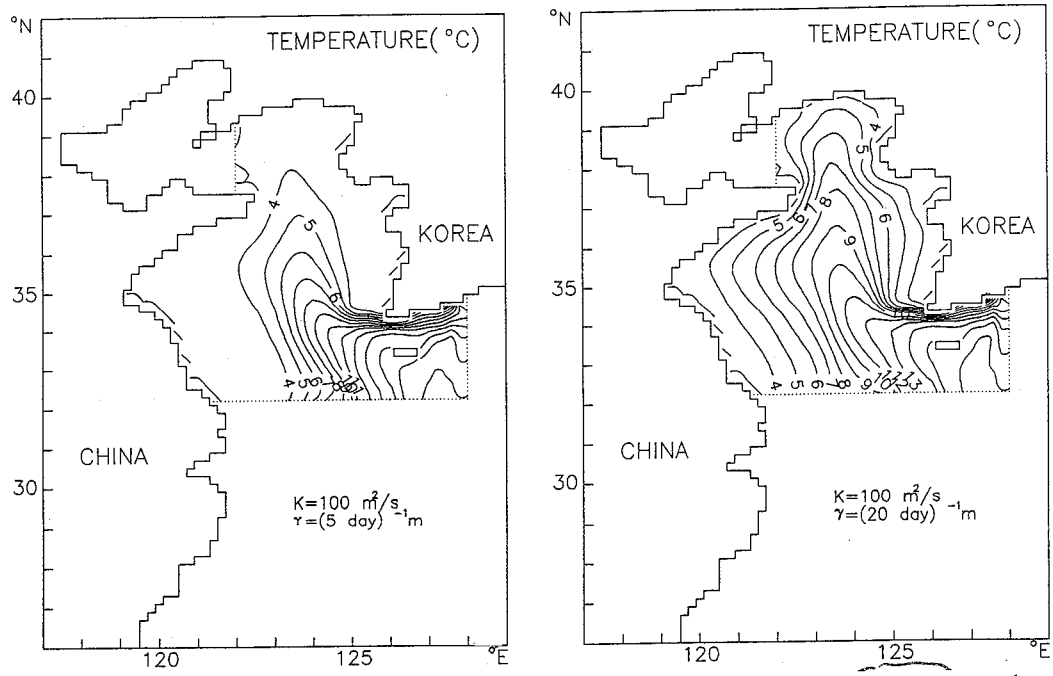

Fig. 7. Distribution of isotherms obtained in the model with cooling coefficients $r=(5\ \text{day})^{-1}$ m and $(20\ \text{day})^{-1}$ m. Others are the same as Fig. 5.

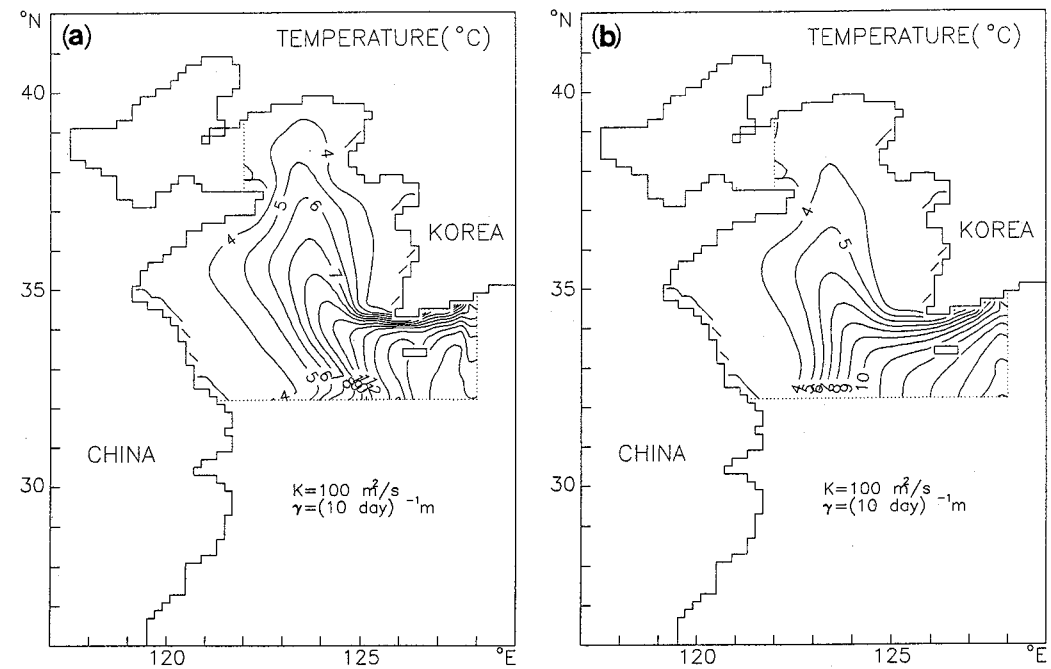

Fig. 8. Distribution of isotherms obtained in the model in cases where a) the Tsushima Current transport is 3.5 Sverdrups and b) there is no Kuroshio/Tsushima Current. Others are the same as Fig. 5. Corresponding stream functions are shown in Fig. 4a and 4b.

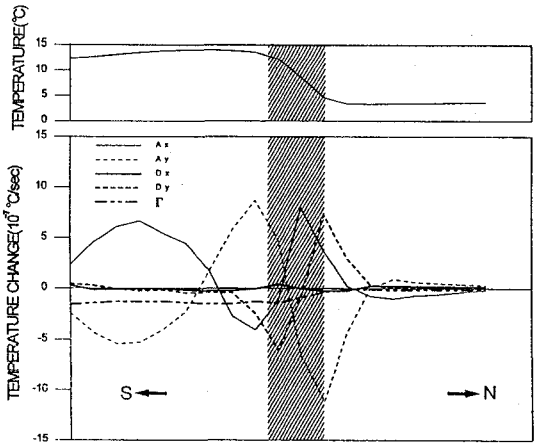

Fig. 9. Temperature profile, and magnitude of each term in the heat equation (6) along the line across the front (see Fig. 5 for the location of the line) for the standard case. N and S mean northward and southward directions respectively and the most intense frontal zone is shaded. Ax means advection in x-direction, Ay advection in y-direction, Dx diffusion in x-direvtion, Dy diffusion in y-direction and Γ local cooling.

flows in the area north of the front. But the latter flows into the front. It will then experience large temperature change near the front. As already observed in Fig. 9, this change is caused by the north-south diffusion.

CONCLUDING REMARKS

A simple model reproduces well the thermo-haline front frequently observed near the southwestern tip of Korean Peninsula. The front is formed when the alongshore cold current driven by prevailing northerly wind encounters the warm water advected from the south by the Tsushima Current. Due to the strong advection by the Tsushima Current, the front occurs north of the Tsushima Current. Since the Tsushima Current approximately follows the isobaths, the front also runs parallel to the isobaths in the east-west direction. In this model, the Tsushima Current plays a dominant role in determining local current and temperature fields since it involves much larger amount of transport than the local wind driven current. It not only advects large amount of heat but also strengthens local current which then changes its path because current tends to follow isobaths as it becomes stronger.

The model considered here is not complete and there are many uncertainties concerning various physical parameters. We are only satisfied with qualitative understanding of the problem. Further detailed studies, both theoretical and experimental, are expected in the near future.

ACKNOWLEDGEMENTS

This study is supported by 1995 research fund of Inha University. Comments from referees are acknowleged.

REFERENCES

Chang, K.I., K. Kim, S.W. Lee and T.B. Shim, 1995. Hydrography and sub-tidal current in the Cheju Strait in Spring, 1983. *J. Korean Soc. Oceanogr.*, **30**: 203-215.

Cho, Y.K. and K. Kim, 1994. Characteristics and origin of the cold water in the South Sea of Korea in Summer. *J. Korean Soc. Oceanogr.*, **29**: 414-421.

Fiadeiro, M.E. and G. Veronis, 1977. On weighted-mean schemes for the finite-difference approximation to the advection-diffusion equation. *Tellus*, **29**: 512-522.

Hsueh, Y., R.D. Romea and P.W. deWitt, 1986. Wintertime winds and coastal sea-level fluctuations in the northeast China Sea, Part II, Numerical model. *J. Phys. Oceanogr.*, **16**: 241-261.

Hsueh, Y., 1988. Recent current observations in the Eastern Yellow Sea. *J. Geophys. Res.*, **93**: 6875-6884.

Korea Ocean Research and Developmrnt Institute, 1987. Oceanographic Atlas of Korean Waters, Vol. **1**: Yellow Sea. 147pp.

Lie, H.J., 1985. Wintertime temperature-salinity characteristics in the southern Hwanghae (Yellow Sea). *J. Oceanogr. Soc. Japan*, **41**: 291-298.

Lim, D.B., 1971. On the origin of the Tsushima current water. *J. Oceanol. Soc. Korea*, **6(2)**: 85-91.

Ministry of Sciences and Technology, Korea, 1993. The exploitation research of marine resources on the Yellow Sea. 827 pp.

Ministry of Sciences and Technology, Korea, 1996. The exploitation research of marine resources on the Yellow Sea. (in press)

Moriyasu, S., 1972. The Tsushima Current. In: Kuroshio: Physical aspects of the Japan current, edited by. Stommel, H. and K. Yoshida, Univ. of Washington Press, Seattle and London, 353-369.

Nakao, T., 1977. Oceanic variability in relation to fisheries in the East China Sea and the Yellow Sea. PhD

Thesis, Tokai Univ., Japan, 637 pp.

Nitani, H., 1972. Beginning of the Kuroshio. In: Kuroshio: Physical aspects of the Japan current, edited by. Stommel, H. and K. Yoshida, Univ. of Washington Press, Seattle and London, 129-163.

Park, Y.H., 1986a. Water characteristics and mouvements of the Yellow Sea Warm Current in summer. *Prog. Oceanogr.*, **17**: 243-254.

Park, Y.H., 1986b. A simple theoretical model for the upwind flow in the southern Yelow Sea. *J. Oceanol. Soc. Korea*, **21**: 203-210.

Qiu, B. and N. Imasato, 1990. A numerical study on the formation of the Kuroshio counter current and the Kuroshio branch current in the East China Sea. *Cont. Shelf Res.*, **10**: 165-184.

Seung, Y.H., 1995. Effect of Shantung Peninsula on the development of mean upwind current in the Yellow Sea. *J. Korean Soc. Oceanogr.*, **30**: 537-542.

Uda, M., 1934. The result of simultaneous oceanographic investigations in the Japan Sea and its adjacent waters in May and June, 1932. *J. Imp. Fish. Exp. Sta.*, **5**: 138-190.

Wells, J.T. and O. K. Huh, 1984. Fall-season patterns of turbidity and sediment transport in the Korea Strait and southeastern Yellow Sea. In: Ocean hydrodynamics of the Japan and East China Seas, edited by. T. Ichiye, Elsevier, Amsterdam, 387-397.

Zheng, Q.A. and V. Klemas, 1982. Determination of winter temperature patterns, fronts andsurface currents in the Yellow Sea and East China Sea from satellite imagery. *Remote Sensing of Environment*, **12**: 201-218.